Acoustic-like waves in non-Maxwellian plasmas

H. Gunell*and F. Skiff

Department of Physics and Astronomy, University of Iowa,

Iowa City, Iowa 52242

Space plasmas in the earth's plasma sheet, in the solar wind and elsewhere often have non-Maxwellian ion velocity distributions. The observed distribution functions contain a plentiful supply of superthermal particles, i.e., particles that are faster than the thermal speed. These are seen as high energy tails having a power-law dependence on velocity.

The simple pole expansion [1, 2, 3] of the distribution function is a sum of simple poles in the complex velocity plane.

$$f(v) = \sum_i \frac{a_i}{v - b_i}, \tag{1}$$

where $f(v)$ is 1 over a truncated Taylor expansion of $\exp(v^2/2)$ multiplied by a mask to model a cutoff in the high energy tails

$$f(v) = M(v)T(v),\ M(v) = \left[1 + \frac{v^2}{2} + \ldots + \frac{1}{m!}(\frac{v^2}{2})^m\right]^{-1},\ T(v) = \left[1 + (\frac{v}{v_0})^{2n}\right]^{-1}. \tag{2}$$

The distribution function can be a sum of terms of the type described by Eq. (2), and functions of other forms can be used as long as $f(v)$ can be written as a finite sum of simple poles according to Eq. (1).

Following the Landau prescription when integrating in the complex plane the dispersion relation for a collisionless plasma with a distribution function described by a simple pole expansion is

$$1 = \sum_\alpha \omega_{p\alpha}^2 \int_{-\infty}^{\infty} \frac{f_\alpha dv}{(\omega - kv)^2} = 2\pi i \sum_\alpha \omega_{p\alpha}^2 \sum_{b_{\alpha i} \in U} \frac{a_{\alpha i}}{(\omega - kb_{\alpha i})^2} \tag{3}$$

where α denotes particle species and U the upper half plane.

It can be shown that for a particle species whose distribution function is an even function of v the Debye length satisfies the relation [2]

$$\frac{1}{\lambda_{D\alpha}^2} = -\omega_{p\alpha}^2 2\pi i \sum_{b_{\alpha i} \in U} \frac{a_{\alpha i}}{b_{\alpha i}^2} \tag{4}$$

When $b_{\alpha i}$ and $a_{\alpha i}$ are the poles and residues of an expansion of the Maxwellian the Debye length of Eq. (4) will approach the Debye length of the Maxwellian as m tends to infinity.

*Email: herbert.gunell@physics.org

Table 1: Debye length λ_{Dm} according to Eq. (4) for expansions found in Eq. (2), for $m = 1, 2, \dots 10$, $n = 0$, are compared with the Debye length λ_D for a Maxwellian that has the same second moment $\langle v^2 \rangle = \sum_{\tilde{b}_i \in U} \tilde{a}_i \tilde{b}_i^2$ as the expansion.

m	2	3	4	5	6	7	8	9	10
$\langle (v/v_t)^2 \rangle$	2.828	1.376	1.137	1.059	1.027	1.013	1.006	1.003	1.002
λ_{Dm}/λ_D	0.6436	0.8750	0.9469	0.9756	0.9884	0.9943	0.9972	0.9986	0.9993

A comparison between the Maxwellian Debye length and the Debye length for the expansion of Eq. (2) is shown in table 1 for various values of m and $n = 0$. In the calculation of λ_{Dm}/λ_D the thermal velocity for the unapproximated Maxwellian is chosen such that both distributions have the same second moment $\langle v^2 \rangle = \sum_{b_i \in U} a_i b_i^2$. For small values of m, i.e., for distributions with an abundance of superthermal particles, the Debye length is significantly smaller than the Debye length of the corresponding Maxwellian. Similar results have been obtained for a kappa-distribution with a small value of kappa [4, 5].

For ion acoustic waves the modulus of the phase velocity $|\omega/k| \ll |\tilde{b}_{ei}|$. Hence the electron term of Eq. (3) is approximately $-1/(k^2\lambda_{De}^2)$, and the dispersion relation becomes

$$1 = \omega_{pi}^2 2\pi i \frac{1}{1 + \frac{1}{k^2\lambda_{De}^2}} \sum_{b_i \in U} \frac{a_i}{(\omega - kb_i)^2}. \tag{5}$$

If a Maxwellian velocity distribution is assumed for the electrons the Debye length $\lambda_{De} = (\epsilon_0 k_{\mathrm{B}} T_{\mathrm{e}}/n_0 q^2)^{1/2}$ that is associated with the Maxwellian can be used. However, when the distribution function is non-Maxwellian but symmetric the Debye length given by Eq. (4) is more appropriate. The dispersion relation can be written as a polynomial in ω/k for a given $k \neq 0$.

$$\prod_i \left(\frac{\omega}{k} - b_i\right)^2 - \frac{\omega_{pi}^2}{k^2} \frac{1}{1 + \frac{1}{k^2\lambda_{De}^2}} 2\pi i \sum_i a_i \prod_{j \neq i} \left(\frac{\omega}{k} - b_j\right)^2 = 0 \tag{6}$$

where the notation $b_i, b_j \in U$, i.e., restriction to the upper half plane, has been omitted in the summation and the products. The difference between Eq. (6) and Löfgren and Gunell's [1] Eq. (7)

$$\prod_i \left(\frac{\omega}{k} - \tilde{b}_i\right)^2 - \frac{\omega_p^2}{k^2} 2\pi i \sum_i \tilde{a}_i \prod_{j \neq i} \left(\frac{\omega}{k} - \tilde{b}_j\right)^2 = 0$$

is the appearance of the new factor $1/(1 + 1/k^2\lambda_{De}^2)$ in the second term on the left hand side of Eq. (6) of this poster. The dispersion relation can be found from Eq. (6) by polynomial root finders in standard numerical packages.

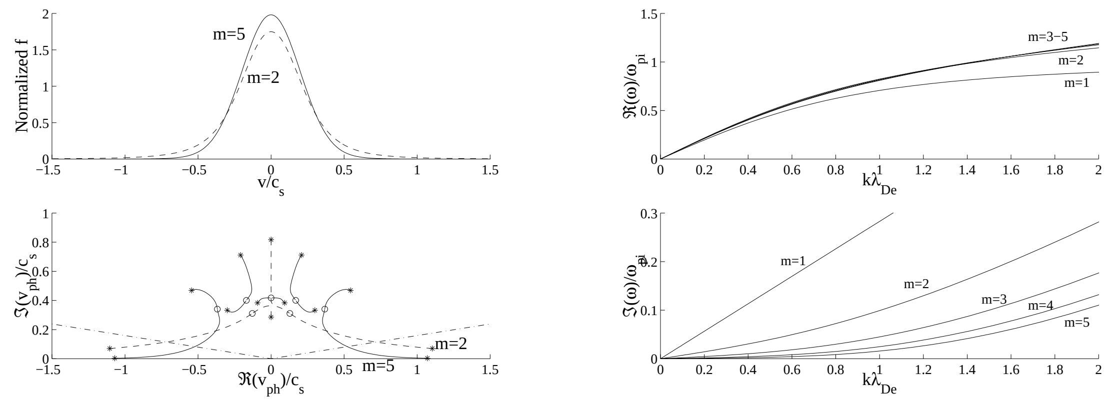

Figure 1: Upper left panel: Expansions of the normalized Maxwellian for $m = 2$ and 5. The ion thermal speed is $v_{ti} = 0.2c_s$, where $c_s = \sqrt{k_B T_e/m_i}$.
Lower left panel: Root paths in the complex phase velocity space for these distribution functions.
Right panels: Dispersion relation for the ion acoustic wave travelling in the positive v direction. The real part of ω is shown as a function of k in the upper panel. The lower panel shows the imaginary part of ω as a function of k.

Ion acoustic waves

An expansion according to Eq. (2) is a good approximation of the Maxwellian at low velocities, but shows increased tails at higher velocities, and can hence be a good approximation to plasmas containing superthermal particles. The normalized distribution function $\tilde{f}_0(v) = f_0(v)/n_0$ for $m = 2$ (dashed curves) and 5 (solid curves), $n = 0$, is shown in the upper left panel of Fig. 1. $T = 1$ for $n = 0$ and there is no high velocity cutoff in the tails. Root paths in the complex phase-velocity space for these distribution functions, are shown in the lower left panel of Fig. 1. The long wavelength limits ($k \to 0$) are marked with stars. As k is increased from zero the roots follow the paths shown and end at a pole of the distribution function as k tends to infinity. The poles are marked with circles. The weakly damped modes are found close to the real axis, and for these distribution functions they can be identified as the ion acoustic waves. For each of the distributions there is one ion acoustic mode propagating in the direction of positive v and one propagating in the direction of negative v. The dash-dotted lines starting at the origin show the border between the weakly and heavily damped regions, with the weakly damped region being below the lines. The criterion used for a wave mode being weakly damped is that the imaginary part of ω shall be less than the real part divided by 2π, i. e., $\Im(\omega)/|\Re(\omega)| < 1/(2\pi)$. In the right panels of Fig. 1 the real (upper right panel) and imaginary (lower right panel) parts of ω are shown as a function of k for the ion acoustic mode travelling in the direction of positive v. The dispersion relations are shown for distributions with $m = 1, 2, 3, 4,$ and 5. Only for the Lorentzian ($m = 1$) is there any significant deviation of the real part of ω from what a true Maxwellian would yield. In the lower panel, however it is seen that superthermal particles contribute significantly to the imaginary part of ω making the wave more damped for small values of m.

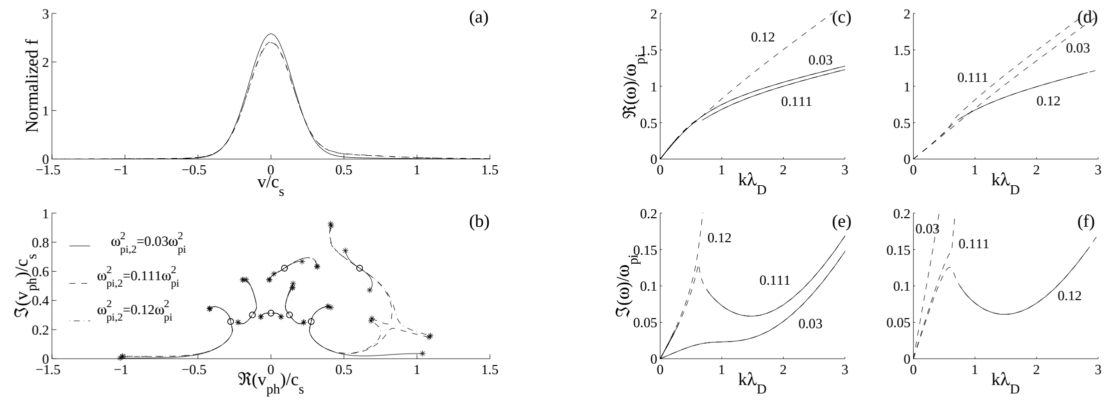

Figure 2: (a) Distribution functions. (b) Root paths in the complex phase velocity space. (c, d) $\Re(\omega)$ and (e, f) $\Im(\omega)$ as a function of k for the most important modes. The dispersion relations for the fast modes are shown in panels (c) and (e), and the slow modes in panels (d) and (f). The words slow and fast here refer to the phase speed in the long wavelength limit ($k \to 0$), which is marked with stars in (b).

Table 2: Parameters of the distribution functions shown in Fig. 2 The total ion plasma frequency ω_{pi} and the sound speed c_s are used as scaling parameters. The background plasma has index 1 and the tail 2.

line	$\omega_{pi,1}^2$	$v_{ti,1}$	$v_{d,1}$	m_1	$\omega_{pi,2}^2$	$v_{ti,2}$	$v_{d,2}$	m_2
—	$0.97\omega_{pi}^2$	$0.15c_s$	0	5	$0.03\omega_{pi}^2$	$0.4c_s$	$0.35c_s$	2
- -	$0.889\omega_{pi}^2$	$0.15c_s$	0	5	$0.111\omega_{pi}^2$	$0.4c_s$	$0.35c_s$	2
-.-	$0.88\omega_{pi}^2$	$0.15c_s$	0	5	$0.12\omega_{pi}^2$	$0.4c_s$	$0.35c_s$	2

Distributions with beam-like tails

In Fig. 2 (a) three distributions with beam-like tails can be seen. A beam-like distribution function is a distribution in which most of the ions belong to a population centred at zero velocity and a fraction of the ions belong to an enhanced tail that can be modeled by an expansion centred at non-zero velocity. Such ion distribution functions have been observed in laboratory plasmas and have been found to carry both classic ion acoustic waves and slow kinetic wave modes [6]. The relative density of the beam (or enhanced tail) shown in Fig. 2 is $\eta = \omega_{pi,2}^2/\omega_{pi}^2 = 0.03$, 0.111, and 0.12 for the three curves respectively. The two distributions with higher tail density are nearly identical. However, the dispersion relations for $\eta = 0.11$ and $\eta = 0.12$ are distinctly different, as Fig. 2 (b) shows. As the relative tail density increases from 0.111 to 0.12 a topological shift occurs, and the ion acoustic mode that for low tail density is connected to a pole of the bulk plasma distribution in stead connects to one of the poles of the tail. For the most important modes travelling in the positive direction ω as a function of k is shown in Fig. 2 (c–f).

All modes shown in Fig. 2 have a constant phase velocity for small k and are hence acoustic-like in their behaviour. Only the traditional ion acoustic mode is weakly damped in the case with the lowest tail density. As the tail density is increased this mode will be weakly damped at small k, strongly damped at intermediate values of k, and have another weakly damped region for larger k. Linear kinetic wave modes differing from the traditional ion acoustic waves have been observed in laboratory experiments [6].

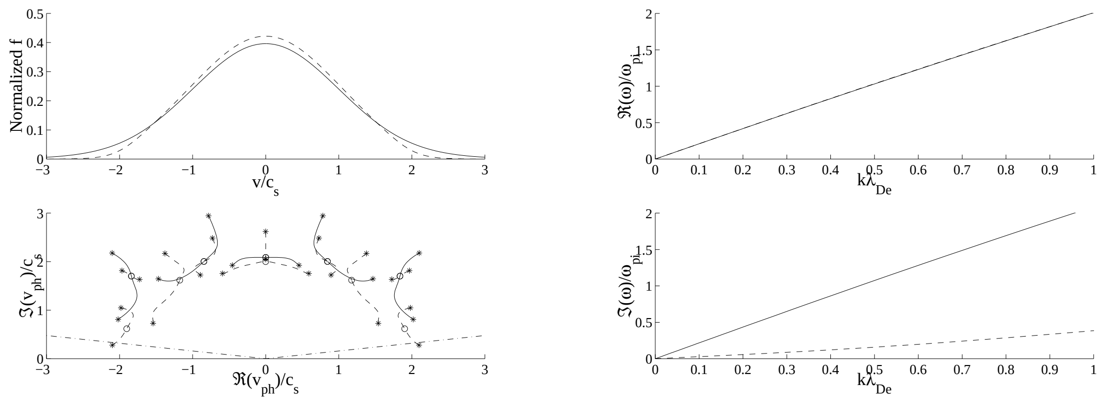

Figure 3: Upper left panel: $m = 5$ expansion of a Maxwellian with $T_i = T_e$ (solid line) and the same function with a gentle cutoff introduced at $v = 2c_s$. Lower left panel: Root paths in the complex phase velocity space for these distributions. The poles of the distribution functions are marked with circles and the limiting solutions $k \to 0$ are marked with stars. Wave modes below the dash-dotted lines in the lower panels fulfill the condition $\Im(\omega)/|\Re(\omega)| < 1/(2\pi)$ and are considered to be weakly damped.
Right panels: Dispersion relation for the least damped acoustic wave travelling in the positive v direction. The real part of ω is shown as a function of k in the upper panel. The lower panel shows the imaginary part of ω as a function of k.

Distributions with cutoffs in the high energy tails

A cutoff in the tail of the distribution can be introduced by setting $n \neq 0$ in Eq. (2). This is equivalent to a multiplication of the expansion with the transfer function of a low-pass Butterworth filter. In Fig. 3 an example of the introduction of a gentle cutoff is shown. In the upper left panel the solid line shows an $m = 5$, $n = 0$ expansion of a Maxwellian distribution function with $T_i = T_e$. The dashed line shows an $m = 5$, $n = 5$ expansion, i.e., the same distribution multiplied by $T(v) = (1 + (v/v_c)^{10})^{-1}$, which is the square of the modulus of the transfer function for a fifth order Butterworth low-pass filter. Here v_c is the cutoff velocity which in the example shown is $2c_s$. This distribution has less ions in the high energy tails. Such a distribution function could be produced in the presence of neutral gas, since the collision frequency for charge-exchange collisions increases with energy. Root paths in the complex phase velocity space for these two distribution functions are shown in the lower left panel of Fig. 3. As expected the Maxwellian plasma with $T_i = T_e$ (solid lines) has only heavily damped modes. For the distribution with the cutoff tails (dashed lines) there is a weakly damped mode with a phase velocity close to $2.1c_s$, which is slightly faster than the cutoff velocity $v_c = 2c_s$. This mode is an acoustic-like mode since, as can be seen in Fig. 3, it has an approximately constant phase speed in the $k \to 0$ limit, which is marked with a star, and hence ω is proportional to k in that limit. It is not, however, a traditional ion acoustic wave as its phase speed is twice the ion sound speed. The introduction of a cutoff decreases the damping at velocities above the cutoff since both the slope of the distribution function and the number of particles in that velocity range decreases when the cutoff is introduced, and Landau damping is proportional to the slope of the distribution function in the neighbourhood of the phase velocity.

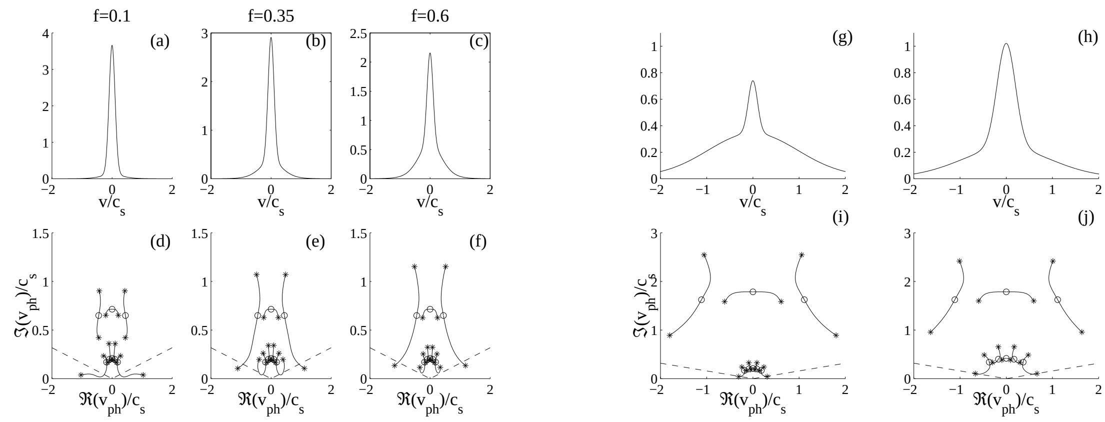

Figure 4: (a–c) Normalized distribution functions. (d–f) Root paths in the complex phase velocity space. Wave modes below the dashed lines in the lower panels fulfill the condition $\Im(\omega)/|\Re(\omega)| < 1/(2\pi)$ and are hence weakly damped. When $f = n_h/n_i = 0.1$ (a,d) the only weakly damped mode is the cold ion acoustic wave. For $f = n_h/n_i = 0.35$ (b,e) the hot ion acoustic wave is weakly damped, and so is the slow (cold) wave for high values of k. At $f = n_h/n_i = 0.6$ the slow wave is heavily damped for all k and the hot acoustic wave is weakly damped. In the three cases shown in (a–f) $m_c = 5$, $v_{tc} = 0.1c_s$, $m_h = 3$, and $v_{th} = 0.4c_s$. Panels (g–j) show the same thing for distributions where $T_e = T_i$ for the hot component. The parameters are $f = 0.9$, $v_{tc} = 0.1c_s$, $v_{th} = c_s$ (g,i) and $f = 0.6$, $v_{tc} = 0.2c_s$, $v_{th} = c_s$ (h,j).

Two-temperature distributions

In a plasma with two ion populations with different temperature weakly damped modes similar to those found in plasmas with beam-like tails exist under some conditions. The different kinds of wave modes that can exist are shown in Fig. 4 (a–f). In the example shown $m_c = 5$, $v_{tc} = 0.1c_s$, $m_h = 3$, and $v_{th} = 0.4c_s$. For low $f = n_h/n_i$ the plasma ions are mostly cold and the cold ion acoustic wave is the only weakly damped wave mode (Fig. 4 (d)). The dashed lines in Fig. 4 (d–f) are the $\Im(\omega)/|\Re(\omega)| = 1/(2\pi)$ lines, that form the border between the weakly and strongly damped regions. Wave modes below the dashed lines are weakly damped. For high f values the dominant wave mode is the ion acoustic wave associated with the hot ion component (Fig. 4 (f)), and for intermediate values of f both the hot and cold waves can be weakly damped (Fig. 4 (e)). The cold wave is strongly damped for small and very large k. For moderately large k there is a regime where a slow weakly damped wave exists.

If the hot ion component is so hot that $T_e = T_i$ there can still be weakly damped modes if a cold ion component is present, and even if that component constitutes only a small fraction of the total ion density. In Fig. 4 (g–j) two examples of this are shown. The three uppermost poles shown in the lower panels are the poles of the hot component of the distribution, for which $v_{th} = c_s$, and hence $T_e = T_i$. The wave modes whose root paths connect to the poles of the hot distribution in the $k \to \infty$ limit are all heavily damped, as would be expected for waves in a plasma with equal electron and ion temperatures. In the presence of a cold plasma component there is a slow weakly damped acoustic wave mode. Its phase speed is lower than the ion sound speed. The slow wave is weakly damped even when the cold ion component only contributes to 10% of the total ion density.

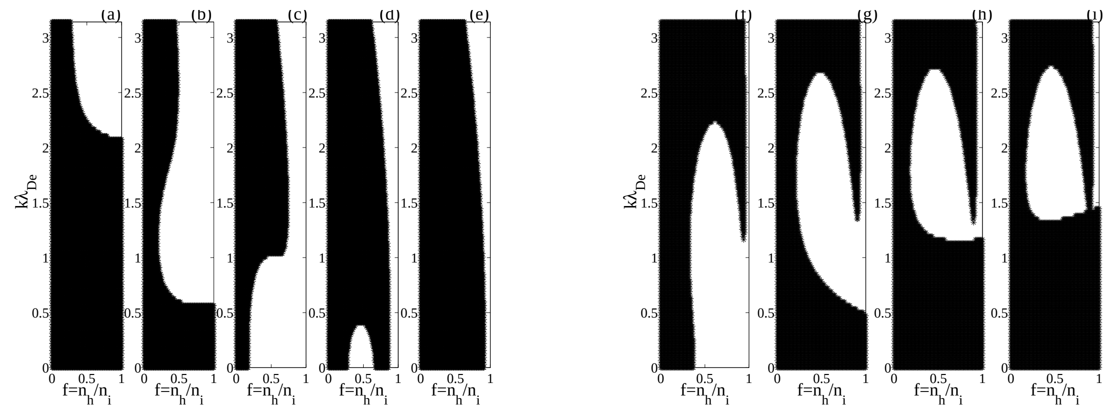

Figure 5: The existence of weakly damped modes for different hot ion temperatures. In the shadowed regions weakly damped ($\Im(\omega)/\Re(\omega) < 1/(2\pi)$) modes exist. In panels (a–e) the cold ions follow a $v_{tc} = 0.1c_s$, $m_c = 5$ expansion, and the hot ions have $m_h = 3$, i.e., a distribution with some superthermal particles. The hot ion thermal speed $v_{th}/c_s = 0.2$, 0.4, 0.6, 0.8, and 1.0 respectively.
In panels (f–i) the cold ions follow a $v_{tc} = 0.03c_s$, $m_c = 5$ expansion, and the hot ions have $v_{th} = 0.3$. The number of superthermal particles decreases as m_h increases. In the four panels $m_h = 1, 2, 3$, and 4 from (f) to (i).

Various parameters of two-temperature plasmas have been investigated to find parameter regimes where weakly damped modes can exist. Fig. 5 (a–e) shows where weakly damped mode exist for a plasma with a cold ion component ($v_{tc} = 0.1c_s$) and a hot component with thermal speeds $v_{th}/c_s = 0.2$, 0.4, 0.6, 0.8, and 1.0 respectively. The diagrams shown in Fig. 5 have been obtained by numerically solving Eq. (5) and applying the weak damping condition $\Im(\omega) < \Re(\omega)/(2\pi)$. In the shadowed regions at least one mode is weakly damped. The shadowed region withdraws from the lower right quadrant of the diagrams as we go from panel (a) to panel (c). This means that as the hot temperature increases the ion acoustic wave associated with the hot ion component gets more damped. Instead a shadow emerges from the upper left corner. This is the slow wave associated with the cold ions, which is weakly damped when v_{th} approaches c_s. The influence of superthermal particles is shown in Fig. 5 (f–i). The cold ions follow a $v_{tc} = 0.03c_s$, $m_c = 5$ expansion, and the hot ions have $v_{th} = 0.3c_s$. The four panels correspond to $m_h = 1, 2, 3$, and 4 from (f) to (i). When m_h is increased from 1 to 4 the number of superthermal particles decreases and the damping of the ion acoustic mode decreases. This is seen in Fig. 5 (f–i) where the shadowed region fills more and more of the lower half of this diagrams as we go from (f) to (i), i. e, towards a lower number of superthermal particles. The existence of a slow mode associated with the cold component is not affected to any great extent of the presence of superthermal particles in the hot ion component.

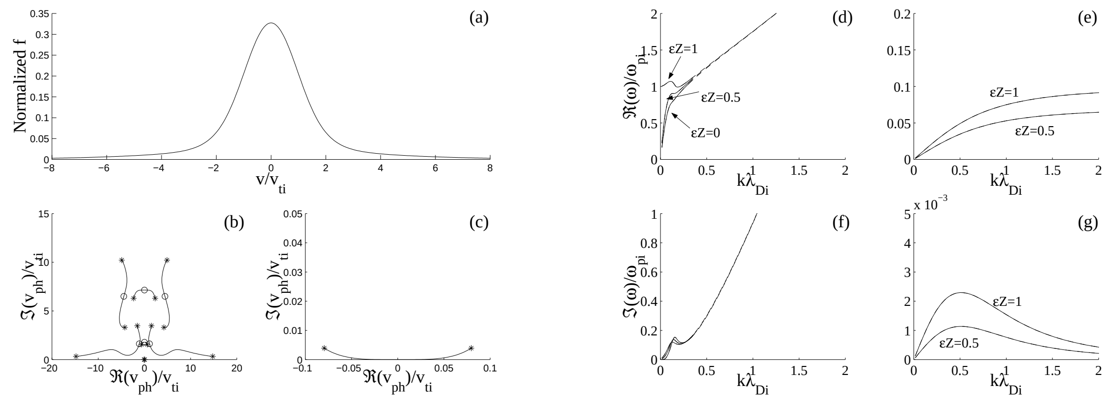

Figure 6: A two-temperature ion distribution function (a), and root paths in the complex phase velocity space (b, c). $\Re(\omega)$ (d, e) and $\Im(\omega)$ (f, g) as functions of k for $\epsilon Z = 0.5$, $\omega_{pd}^2 = 0.01\omega_{pi}^2 \cdot \epsilon Z$. Panel (c) shows the dust acoustic wave on a larger scale. Panels (d–g) show $\epsilon Z = 0$, 0.5, and 1.

Waves in dusty plasmas

The simple pole expansion can also be used to study waves in collisionless dusty plasmas. Assuming that the dust is cold and the electrons are hot ($|b_{di}| \ll |\omega/k| \ll |b_{ei}|$) Eq. (3) can be simplified to

$$1 = \frac{\omega_{pd}^2}{\omega^2} - \frac{1}{k^2\lambda_{De}^2} + \omega_{pi}^2 2\pi i \sum_{b_{ii}\in U} \frac{a_{ii}}{(\omega - kb_{ii})^2}. \tag{7}$$

Assuming singly charged positive ions, and negatively charge dust, ϵZ is the fraction of the negative charge that resides on the dust grains when $\epsilon = n_d/n_i$ is the dust to ion density ratio and $-Ze$ is the dust grain charge. Hence $n_e = (1 - \epsilon Z)n_i$, $\omega_{pd}^2 = \omega_{pi}^2 \left(m_i/\left(m_d\epsilon\right)\right)\left(\epsilon Z\right)^2$, and $\lambda_{De}^2 = \lambda_{Di}^2 T_e/\left(T_i\left(1 - eZ\right)\right)$.

In Fig. 6 (b, c) the dispersion relation is shown for $\epsilon Z = 0.5$, $\omega_{pd}^2 = 0.01\omega_{pi}^2 \cdot \epsilon Z$. The two components of the ion distribution have $v_{ti1} = v_{ti}$, $\omega_{pi1}^2 = 0.81\omega_{pi}^2$, and $v_{ti2} = 4v_{ti}$, $\omega_{pi2}^2 = 0.19\omega_{pi}^2$ respectively. As half of the negative charge is confined to the cold dust grains the electrons can not shield the ions as effectively as they do in the absence of dust. This makes the dust ion acoustic wave faster than the ion acoustic wave. If all the negative charge is on the dust grains and there are no free electrons the phase speed of the dust ion acoustic wave will tend to infinity as $k \to 0$, and the dust ion acoustic wave will then be analogous with an electron wave in a two electron temperature plasma, where electrons correspond to the ions in the dust ion acoustic waves, and the ions of the electron wave correspond to the heavy dust grains of the dust ion acoustic wave. That is to say the particles of the heaviest species do nothing else than provide a background of neutralising charge.

When the dust grains are included in this way effects of the dust velocity distribution and dust charging processes are not taken into account. The dispersion relations for the dust acoustic wave could hence be inaccurate. The results for the dust ion acoustic wave are still valid, because their frequency is much higher than the dust plasma frequency.

Summary

- Using a simple pole expansion we have calculated λ_D for $f(v)$, symmetric around $v = 0$, and derived an equation for the dispersion relation for waves on an ion acoustic time scale ($|\omega/k| \ll v_{te}$).
- Slow ($v_{ph} < c_s$) weakly damped acoustic-like waves are found for
  - Two-component distributions with beam-like tails
  - Two-component two-temperature distributions
- This happens even when $T_e = T_i$.
- For one component distribution functions with $T_e = T_i$ weakly damped modes are found when a cutoff appears in the tails. Its phase velocity is close to the cutoff velocity.
- In a classic ion acoustic wave the electrons provide shielding for the ions. In a two ion temperature plasma the hot ions assume the role of the electrons, shielding the cold ions, and hence a slow weakly damped acoustic-like wave can exist. The damping decreases further if the hot ions have a non-zero mean velocity (beam-like tails). Similar modes appear in plasmas with two ion species, and in plasmas with two electron temperatures.
- These weakly damped wave modes have been found in laboratory experiments and are likely to occur in space plasmas, where distributions of this kind are common.
- The simple pole expansion can also be used to study waves in dusty plasmas.

References

[1] T. Löfgren and H. Gunell, "Flexible simple-pole expansion of distribution functions," *Physics of Plasmas*, vol. 4, pp. 3469–3476, 1997.

[2] H. Gunell and F. Skiff, "Weakly damped acoustic-like ion waves in plasmas with non-maxwellian ion distributions," *Physics of Plasmas*, vol. 8, pp. 3550–3557, 2001.

[3] A. Tjulin, A. I. Eriksson, and M. André, "Physical interpretation of the Padé approximation of the plasma dispersion function," *Journal of Plasma Physics*, vol. 64, pp. 287–296, 2000.

[4] D. A. Bryant, "Debye length in a kappa-distribution plasma," *Journal of Plasma Physics*, vol. 56, pp. 87–93, 1996.

[5] R. L. Mace, M. A. Hellberg, and R. A. Treumann, "Electrostatic fluctuations in plasmas containing suprathermal particles," *Journal of Plasma Physics*, vol. 59, pp. 393–416, 1998.

[6] F. Skiff, S. De Souza-Machado, W. A. Noonan, A. Case, and T. N. Good, "Linear kinetic modes in weakly collisional plasma," *Physical Review Letters*, vol. 81, no. 26, pp. 5820–5823, 1998.